Measurements of Absolute Hadronic Branching Fractions of the Λ_c^+ Baryon

M. Ablikim,[1] M. N. Achasov,[9,e] X. C. Ai,[1] O. Albayrak,[5] M. Albrecht,[4] D. J. Ambrose,[44] A. Amoroso,[49a,49c] F. F. An,[1] Q. An,[46,a] J. Z. Bai,[1] R. Baldini Ferroli,[20a] Y. Ban,[31] D. W. Bennett,[19] J. V. Bennett,[5] M. Bertani,[20a] D. Bettoni,[21a] J. M. Bian,[43] F. Bianchi,[49a,49c] E. Boger,[23,c] I. Boyko,[23] R. A. Briere,[5] H. Cai,[51] X. Cai,[1,a] O. Cakir,[40a] A. Calcaterra,[20a] G. F. Cao,[1] S. A. Cetin,[40b] J. F. Chang,[1,a] G. Chelkov,[23,c,d] G. Chen,[1] H. S. Chen,[1] H. Y. Chen,[2] J. C. Chen,[1] M. L. Chen,[1,a] S. J. Chen,[29] X. Chen,[1,a] X. R. Chen,[26] Y. B. Chen,[1,a] H. P. Cheng,[17] X. K. Chu,[31] G. Cibinetto,[21a] H. L. Dai,[1,a] J. P. Dai,[34] A. Dbeyssi,[14] D. Dedovich,[23] Z. Y. Deng,[1] A. Denig,[22] I. Denysenko,[23] M. Destefanis,[49a,49c] F. De Mori,[49a,49c] Y. Ding,[27] C. Dong,[30] J. Dong,[1,a] L. Y. Dong,[1] M. Y. Dong,[1,a] Z. L. Dou,[29] S. X. Du,[53] P. F. Duan,[1] E. E. Eren,[40b] J. Z. Fan,[39] J. Fang,[1,a] S. S. Fang,[1] X. Fang,[46,a] Y. Fang,[1] R. Farinelli,[21a,21b] L. Fava,[49b,49c] O. Fedorov,[23] F. Feldbauer,[22] G. Felici,[20a] C. Q. Feng,[46,a] E. Fioravanti,[21a] M. Fritsch,[14,22] C. D. Fu,[1] Q. Gao,[1] X. L. Gao,[46,a] X. Y. Gao,[2] Y. Gao,[39] Z. Gao,[46,a] I. Garzia,[21a] K. Goetzen,[10] L. Gong,[30] W. X. Gong,[1,a] W. Gradl,[22] M. Greco,[49a,49c] M. H. Gu,[1,a] Y. T. Gu,[12] Y. H. Guan,[1] A. Q. Guo,[1] L. B. Guo,[28] Y. Guo,[1] Y. P. Guo,[22] Z. Haddadi,[25] A. Hafner,[22] S. Han,[51] X. Q. Hao,[15] F. A. Harris,[42] K. L. He,[1] T. Held,[4] Y. K. Heng,[1,a] Z. L. Hou,[1] C. Hu,[28] H. M. Hu,[1] J. F. Hu,[49a,49c] T. Hu,[1,a] Y. Hu,[1] G. S. Huang,[46,a] J. S. Huang,[15] X. T. Huang,[33] Y. Huang,[29] T. Hussain,[48] Q. Ji,[1] Q. P. Ji,[30] X. B. Ji,[1] X. L. Ji,[1,a] L. W. Jiang,[51] X. S. Jiang,[1,a] X. Y. Jiang,[30] J. B. Jiao,[33] Z. Jiao,[17] D. P. Jin,[1,a] S. Jin,[1] T. Johansson,[50] A. Julin,[43] N. Kalantar-Nayestanaki,[25] X. L. Kang,[1] X. S. Kang,[30] M. Kavatsyuk,[25] B. C. Ke,[5] P. Kiese,[22] R. Kliemt,[14] B. Kloss,[22] O. B. Kolcu,[40b,h] B. Kopf,[4] M. Kornicer,[42] W. Kuehn,[24] A. Kupsc,[50] J. S. Lange,[24,a] M. Lara,[19] P. Larin,[14] C. Leng,[49c] C. Li,[50] Cheng Li,[46,a] D. M. Li,[53] F. Li,[1,a] F. Y. Li,[31] G. Li,[1] H. B. Li,[1] J. C. Li,[1] Jin Li,[32] K. Li,[13] K. Li,[33] Lei Li,[3] P. R. Li,[41,i] Q. Y. Li,[33] T. Li,[33] W. D. Li,[1] W. G. Li,[1] X. L. Li,[33] X. M. Li,[12] X. N. Li,[1,a] X. Q. Li,[30] Z. B. Li,[38] H. Liang,[46,a] Y. F. Liang,[36] Y. T. Liang,[24] G. R. Liao,[11] D. X. Lin,[14] B. J. Liu,[1] C. X. Liu,[1] D. Liu,[46,a] F. H. Liu,[35] Fang Liu,[1] Feng Liu,[6] H. B. Liu,[12] H. H. Liu,[1] H. H. Liu,[16] H. M. Liu,[1] J. Liu,[1] J. B. Liu,[46,a] J. P. Liu,[51] J. Y. Liu,[1] K. Liu,[39] K. Y. Liu,[27] L. D. Liu,[31] P. L. Liu,[1,a] Q. Liu,[41] S. B. Liu,[46,a] X. Liu,[26] Y. B. Liu,[30] Z. A. Liu,[1,a] Zhiqing Liu,[22] H. Loehner,[25] X. C. Lou,[1,a,g] H. J. Lu,[17] J. G. Lu,[1,a] Y. Lu,[1] Y. P. Lu,[1,a] C. L. Luo,[28] M. X. Luo,[52] T. Luo,[42] X. L. Luo,[1,a] X. R. Lyu,[41,j] F. C. Ma,[27] H. L. Ma,[1] L. L. Ma,[33] Q. M. Ma,[1] T. Ma,[1] X. N. Ma,[30] X. Y. Ma,[1,a] Y. M. Ma,[33] F. E. Maas,[14] M. Maggiora,[49a,49c] Y. J. Mao,[31] Z. P. Mao,[1] S. Marcello,[49a,49c] J. G. Messchendorp,[25] J. Min,[1,a] R. E. Mitchell,[19] X. H. Mo,[1,a] Y. J. Mo,[6] C. Morales Morales,[14] N. Yu. Muchnoi,[9,e] H. Muramatsu,[43] Y. Nefedov,[23] F. Nerling,[14] I. B. Nikolaev,[9,e] Z. Ning,[1,a] S. Nisar,[8] S. L. Niu,[1,a] X. Y. Niu,[1] S. L. Olsen,[32] Q. Ouyang,[1,a] S. Pacetti,[20b] Y. Pan,[46,a] P. Patteri,[20a] M. Pelizaeus,[4] H. P. Peng,[46,a] K. Peters,[10] J. Pettersson,[50] J. L. Ping,[28] R. G. Ping,[1] R. Poling,[43] V. Prasad,[1] H. R. Qi,[2] M. Qi,[29] S. Qian,[1,a] C. F. Qiao,[41] L. Q. Qin,[33] N. Qin,[51] X. S. Qin,[1] Z. H. Qin,[1,a] J. F. Qiu,[1] K. H. Rashid,[48] C. F. Redmer,[22] M. Ripka,[22] G. Rong,[1] Ch. Rosner,[14] X. D. Ruan,[12] V. Santoro,[21a] A. Sarantsev,[23,f] M. Savrié,[21b] K. Schoenning,[50] S. Schumann,[22] W. Shan,[31] M. Shao,[46,a] C. P. Shen,[2] P. X. Shen,[30] X. Y. Shen,[1] H. Y. Sheng,[1] W. M. Song,[1] X. Y. Song,[1] S. Sosio,[49a,49c] S. Spataro,[49a,49c] G. X. Sun,[1] J. F. Sun,[15] S. S. Sun,[1] Y. J. Sun,[46,a] Y. Z. Sun,[1] Z. J. Sun,[1,a] Z. T. Sun,[19] C. J. Tang,[36] X. Tang,[1] I. Tapan,[40c] E. H. Thorndike,[44] M. Tiemens,[25] M. Ullrich,[24] I. Uman,[40d] G. S. Varner,[42] B. Wang,[30] B. L. Wang,[41] D. Wang,[31] D. Y. Wang,[31] K. Wang,[1,a] L. L. Wang,[1] L. S. Wang,[1] M. Wang,[33] P. Wang,[1] P. L. Wang,[1] S. G. Wang,[31] W. Wang,[1,a] W. P. Wang,[46,a] X. F. Wang,[39] Y. D. Wang,[14] Y. F. Wang,[1,a] Y. Q. Wang,[22] Z. Wang,[1,a] Z. G. Wang,[1,a] Z. H. Wang,[46,a] Z. Y. Wang,[1] T. Weber,[22] D. H. Wei,[11] J. B. Wei,[31] P. Weidenkaff,[22] S. P. Wen,[1] U. Wiedner,[4] M. Wolke,[50] L. H. Wu,[1] Z. Wu,[1,a] L. Xia,[46,a] L. G. Xia,[39] Y. Xia,[18] D. Xiao,[1] H. Xiao,[47] Z. J. Xiao,[28] Y. G. Xie,[1,a] Q. L. Xiu,[1,a] G. F. Xu,[1] L. Xu,[1] Q. J. Xu,[13] Q. N. Xu,[41] X. P. Xu,[37] L. Yan,[49a,49c] W. B. Yan,[46,a] W. C. Yan,[46,a] Y. H. Yan,[18] H. J. Yang,[34] H. X. Yang,[1] L. Yang,[51] Y. X. Yang,[11] M. Ye,[1,a] M. H. Ye,[7] J. H. Yin,[1] B. X. Yu,[1,a] C. X. Yu,[30] J. S. Yu,[26] C. Z. Yuan,[1] W. L. Yuan,[29] Y. Yuan,[1] A. Yuncu,[40b,b] A. A. Zafar,[48] A. Zallo,[20a] Y. Zeng,[18] Z. Zeng,[46,a] B. X. Zhang,[1] B. Y. Zhang,[1,a] C. Zhang,[29] C. C. Zhang,[1] D. H. Zhang,[1] H. H. Zhang,[38] H. Y. Zhang,[1,a] J. J. Zhang,[1] J. L. Zhang,[1] J. Q. Zhang,[1] J. W. Zhang,[1,a] J. Y. Zhang,[1] J. Z. Zhang,[1] K. Zhang,[1] L. Zhang,[1] X. Y. Zhang,[33] Y. Zhang,[1] Y. H. Zhang,[1,a] Y. N. Zhang,[41] Y. T. Zhang,[46,a] Yu Zhang,[41] Z. H. Zhang,[6] Z. P. Zhang,[46] Z. Y. Zhang,[51] G. Zhao,[1] J. W. Zhao,[1,a] J. Y. Zhao,[1] J. Z. Zhao,[1,a] Lei Zhao,[46,a] Ling Zhao,[1] M. G. Zhao,[30] Q. Zhao,[1] Q. W. Zhao,[1] S. J. Zhao,[53] T. C. Zhao,[1] Y. B. Zhao,[1,a] Z. G. Zhao,[46,a] A. Zhemchugov,[23,c] B. Zheng,[47] J. P. Zheng,[1,a] W. J. Zheng,[33] Y. H. Zheng,[41] B. Zhong,[28] L. Zhou,[1,a] X. Zhou,[51] X. K. Zhou,[46,a] X. R. Zhou,[46,a] X. Y. Zhou,[1] K. Zhu,[1] K. J. Zhu,[1,a] S. Zhu,[1] S. H. Zhu,[45] X. L. Zhu,[39] Y. C. Zhu,[46,a] Y. S. Zhu,[1] Z. A. Zhu,[1] J. Zhuang,[1,a] L. Zotti,[49a,49c] B. S. Zou,[1] and J. H. Zou[1]

(BESIII Collaboration)

[1]*Institute of High Energy Physics, Beijing 100049, People's Republic of China*
[2]*Beihang University, Beijing 100191, People's Republic of China*
[3]*Beijing Institute of Petrochemical Technology, Beijing 102617, People's Republic of China*
[4]*Bochum Ruhr-University, D-44780 Bochum, Germany*
[5]*Carnegie Mellon University, Pittsburgh, Pennsylvania 15213, USA*
[6]*Central China Normal University, Wuhan 430079, People's Republic of China*
[7]*China Center of Advanced Science and Technology, Beijing 100190, People's Republic of China*
[8]*COMSATS Institute of Information Technology, Lahore, Defence Road, Off Raiwind Road, 54000 Lahore, Pakistan*
[9]*G.I. Budker Institute of Nuclear Physics SB RAS (BINP), Novosibirsk 630090, Russia*
[10]*GSI Helmholtzcentre for Heavy Ion Research GmbH, D-64291 Darmstadt, Germany*
[11]*Guangxi Normal University, Guilin 541004, People's Republic of China*
[12]*GuangXi University, Nanning 530004, People's Republic of China*
[13]*Hangzhou Normal University, Hangzhou 310036, People's Republic of China*
[14]*Helmholtz Institute Mainz, Johann-Joachim-Becher-Weg 45, D-55099 Mainz, Germany*
[15]*Henan Normal University, Xinxiang 453007, People's Republic of China*
[16]*Henan University of Science and Technology, Luoyang 471003, People's Republic of China*
[17]*Huangshan College, Huangshan 245000, People's Republic of China*
[18]*Hunan University, Changsha 410082, People's Republic of China*
[19]*Indiana University, Bloomington, Indiana 47405, USA*
[20a]*INFN Laboratori Nazionali di Frascati, I-00044 Frascati, Italy*
[20b]*INFN and University of Perugia, I-06100, Perugia, Italy*
[21a]*INFN Sezione di Ferrara, I-44122 Ferrara, Italy*
[21b]*University of Ferrara, I-44122 Ferrara, Italy*
[22]*Johannes Gutenberg University of Mainz, Johann-Joachim-Becher-Weg 45, D-55099 Mainz, Germany*
[23]*Joint Institute for Nuclear Research, 141980 Dubna, Moscow region, Russia*
[24]*Justus Liebig University Giessen, II. Physikalisches Institut, Heinrich-Buff-Ring 16, D-35392 Giessen, Germany*
[25]*KVI-CART, University of Groningen, NL-9747 AA Groningen, Netherlands*
[26]*Lanzhou University, Lanzhou 730000, People's Republic of China*
[27]*Liaoning University, Shenyang 110036, People's Republic of China*
[28]*Nanjing Normal University, Nanjing 210023, People's Republic of China*
[29]*Nanjing University, Nanjing 210093, People's Republic of China*
[30]*Nankai University, Tianjin 300071, People's Republic of China*
[31]*Peking University, Beijing 100871, People's Republic of China*
[32]*Seoul National University, Seoul 151-747 Korea*
[33]*Shandong University, Jinan 250100, People's Republic of China*
[34]*Shanghai Jiao Tong University, Shanghai 200240, People's Republic of China*
[35]*Shanxi University, Taiyuan 030006, People's Republic of China*
[36]*Sichuan University, Chengdu 610064, People's Republic of China*
[37]*Soochow University, Suzhou 215006, People's Republic of China*
[38]*Sun Yat-Sen University, Guangzhou 510275, People's Republic of China*
[39]*Tsinghua University, Beijing 100084, People's Republic of China*
[40a]*Ankara University, 06100 Tandogan, Ankara, Turkey*
[40b]*Istanbul Bilgi University, 34060 Eyup, Istanbul, Turkey*
[40c]*Uludag University, 16059 Bursa, Turkey*
[40d]*Near East University, Nicosia, North Cyprus, Mersin 10, Turkey*
[41]*University of Chinese Academy of Sciences, Beijing 100049, People's Republic of China*
[42]*University of Hawaii, Honolulu, Hawaii 96822, USA*
[43]*University of Minnesota, Minneapolis, Minnesota 55455, USA*
[44]*University of Rochester, Rochester, New York 14627, USA*
[45]*University of Science and Technology Liaoning, Anshan 114051, People's Republic of China*
[46]*University of Science and Technology of China, Hefei 230026, People's Republic of China*
[47]*University of South China, Hengyang 421001, People's Republic of China*
[48]*University of the Punjab, Lahore-54590, Pakistan*
[49a]*University of Turin, I-10125 Turin, Italy*
[49b]*University of Eastern Piedmont, I-15121, Alessandria, Italy*
[49c]*INFN, I-10125 Turin, Italy*
[50]*Uppsala University, Box 516, SE-75120 Uppsala, Sweden*
[51]*Wuhan University, Wuhan 430072, People's Republic of China*
[52]*Zhejiang University, Hangzhou 310027, People's Republic of China*
[53]*Zhengzhou University, Zhengzhou 450001, People's Republic of China*

We report the first measurement of absolute hadronic branching fractions of Λ_c^+ baryon at the $\Lambda_c^+\bar{\Lambda}_c^-$ production threshold, in the 30 years since the Λ_c^+ discovery. In total, 12 Cabibbo-favored Λ_c^+ hadronic decay modes are analyzed with a double-tag technique, based on a sample of 567 pb^{-1} of e^+e^- collisions at $\sqrt{s} = 4.599$ GeV recorded with the BESIII detector. A global least-squares fitter is utilized to improve the measured precision. Among the measurements for twelve Λ_c^+ decay modes, the branching fraction for $\Lambda_c^+ \to pK^-\pi^+$ is determined to be $(5.84 \pm 0.27 \pm 0.23)\%$, where the first uncertainty is statistical and the second is systematic. In addition, the measurements of the branching fractions of the other 11 Cabibbo-favored hadronic decay modes are significantly improved.

Charmed baryon decays provide crucial information for the study of both strong and weak interactions. Hadronic decays of Λ_c^+, the lightest charmed baryon with quark configuration udc, provide important input to Λ_b physics as Λ_b decays dominantly to Λ_c^+ [1,2]. Improved measurements of the Λ_c^+ hadronic decays can be used to constrain fragmentation functions of charm and bottom quarks by counting inclusive heavy flavor baryons [3]. Most Λ_c^+ branching fractions (BF) have until now been obtained by combining measurements of ratios with a single branching fraction of the *golden* reference mode $\Lambda_c^+ \to pK^-\pi^+$, thus introducing strong correlations and compounding uncertainties. The experimentally averaged BF, $\mathcal{B}(\Lambda_c^+ \to pK^-\pi^+) = (5.0 \pm 1.3)\%$ [4], has large uncertainty due to the introduction of model assumptions on Λ_c^+ inclusive decays in these measurements [5]. Recently, the Belle experiment reported $\mathcal{B}(\Lambda_c^+ \to pK^-\pi^+) = (6.84 \pm 0.24^{+0.21}_{-0.27})\%$ with a precision improved by a factor of 5 over previous results [6]. However, most hadronic BFs still have poor precision [4]. In this Letter, we present the first simultaneous determination of multiple Λ_c^+ absolute BFs.

Our analysis is based on a data sample with an integrated luminosity of 567 pb^{-1} [7] collected with the BESIII detector [8] at the center-of-mass energy of $\sqrt{s} = 4.599$ GeV. At this energy, no additional hadrons accompanying the $\Lambda_c^+\bar{\Lambda}_c^-$ pairs are produced. Previously, the Mark III collaboration measured D hadronic BFs at the $D\bar{D}$ threshold using a double-tag technique, which relies on fully reconstructing both D and $\bar{D}$ decays [9]. This technique obviates the need for knowledge of the luminosity or the production cross section. We employ a similar technique [10] using BESIII data near the $\Lambda_c^+\bar{\Lambda}_c^-$ threshold, resulting in improved measurements of charge-averaged BFs for 12 Cabibbo-favored hadronic decay modes: $\Lambda_c^+ \to pK_S^0$, $pK^-\pi^+$, $pK_S^0\pi^0$, $pK_S^0\pi^+\pi^-$, $pK^-\pi^+\pi^0$, $\Lambda\pi^+$, $\Lambda\pi^+\pi^0$, $\Lambda\pi^+\pi^-\pi^+$, $\Sigma^0\pi^+$, $\Sigma^+\pi^0$, $\Sigma^+\pi^+\pi^-$, and $\Sigma^+\omega$ [11]. Throughout the Letter, charge-conjugate modes are implicitly assumed, unless otherwise stated.

To identify the $\Lambda_c^+\bar{\Lambda}_c^-$ signal candidates, we first reconstruct one $\bar{\Lambda}_c^-$ baryon [called a single tag (ST)] through the final states of any of the 12 modes. For a given decay mode j, the ST yield is determined to be

$$N_j^{\mathrm{ST}} = N_{\Lambda_c^+\bar{\Lambda}_c^-}\mathcal{B}_j\varepsilon_j, \qquad (1)$$

where $N_{\Lambda_c^+\bar{\Lambda}_c^-}$ is the total number of produced $\Lambda_c^+\bar{\Lambda}_c^-$ pairs and ε_j is the corresponding efficiency. Then we define double-tag (DT) events as those where the partner Λ_c^+ recoiling against the $\bar{\Lambda}_c^-$ is reconstructed in one of the 12 modes. That is, in DT events, the $\Lambda_c^+\bar{\Lambda}_c^-$ event is fully reconstructed. The DT yield with $\Lambda_c^+ \to i$ (signal mode) and $\bar{\Lambda}_c^- \to j$ (tagging mode) is

$$N_{ij}^{\mathrm{DT}} = N_{\Lambda_c^+\bar{\Lambda}_c^-}\mathcal{B}_i\mathcal{B}_j\varepsilon_{ij}, \qquad (2)$$

where ε_{ij} is the efficiency for simultaneously reconstructing modes i and j. Hence, the ratio of the DT yield (N_{ij}^{DT}) and ST yield (N_j^{ST}) provides an absolute measurement of the BF:

$$\mathcal{B}_i = \frac{N_{ij}^{\mathrm{DT}}}{N_j^{\mathrm{ST}}}\frac{\varepsilon_j}{\varepsilon_{ij}}. \qquad (3)$$

Because of the large acceptance of the BESIII detector and the low multiplicities of Λ_c hadronic decays, $\varepsilon_{ij} \approx \varepsilon_i\varepsilon_j$. Hence, the ratio $\varepsilon_j/\varepsilon_{ij}$ is insensitive to most systematic effects associated with the decay mode j, and a signal BF $\mathcal{B}_i$ obtained using this procedure is nearly independent of the efficiency of the tagging mode. Therefore, $\mathcal{B}_i$ is sensitive to the signal mode efficiency (ε_i), whose uncertainties dominate the contribution to the systematic error from the efficiencies. According to Eqs. (1) and (2), the total DT yield with $\Lambda_c^+ \to i$ (signal mode) over the 12 ST modes is determined to be

$$N_{i-}^{\mathrm{DT}} = N_{\Lambda_c^+\bar{\Lambda}_c^-}\sum_j \mathcal{B}_i\mathcal{B}_j\varepsilon_{i-}^{\mathrm{DT}}, \qquad (4)$$

where $\varepsilon_{i-}^{\mathrm{DT}} \equiv [\sum_j(\mathcal{B}_j\varepsilon_{ij})/\sum_j\mathcal{B}_j]$ is the average DT efficiency weighted over the 12 modes.

The BESIII detector is an approximately cylindrically symmetric detector with 93% coverage of the solid angle around the e^+e^- interaction point (IP). The components of the apparatus, ordered by distance from the IP, are a 43-layer small-cell main drift chamber (MDC), a time-of-flight (TOF) system based on plastic scintillators with

two layers in the barrel region and one layer in the end-cap region, a 6240-cell CsI(Tl) crystal electromagnetic calorimeter (EMC), a superconducting solenoid magnet providing a 1.0 T magnetic field aligned with the beam axis, and resistive-plate muon-counter layers interleaved with steel. The momentum resolution for charged tracks in the MDC is 0.5% for a transverse momentum of 1 GeV/c. The energy resolution in the EMC is 2.5% in the barrel region and 5.0% in the end-cap region for 1 GeV photons. Particle identification (PID) for charged tracks combines measurements of the energy deposit dE/dx in MDC and flight time in TOF and forms likelihoods $\mathcal{L}(h)(h = p, K, \pi)$ for a hadron h hypothesis. More details about the BESIII detector are provided elsewhere [8].

High-statistics Monte Carlo (MC) simulations of e^+e^- annihilations are used to understand backgrounds and to estimate detection efficiencies. The simulation includes the beam-energy spread and initial-state radiation (ISR) of the e^+e^- collisions as simulated with KKMC [12]. The inclusive MC sample consists of $\Lambda_c^+\bar{\Lambda}_c^-$ events, $D_{(s)}$ production [13], ISR return to lower-mass ψ states, and continuum processes $e^+e^- \to q\bar{q}(q = u, d, s)$. Decay modes as specified in the Particle Data Group summary (PDG) [4] are modeled with EVTGEN [14]. For the MC production of $e^+e^- \to \Lambda_c^+\bar{\Lambda}_c^-$, the observed cross sections are taken into account, and phase-space-generated Λ_c^+ decays are reweighted according to the observed behaviors in data. All final tracks and photons are fed into a GEANT4-based [15] detector simulation package.

Charged tracks detected in the MDC must satisfy $|\cos\theta| < 0.93$ (where θ is the polar angle with respect to the beam direction) and have a distance of closest approach to the IP of less than 10 cm along the beam axis and less than 1 cm in the perpendicular plane, except for those used for reconstructing K_S^0 and Λ decays. Tracks are identified as protons when the PID determines this hypothesis to have the greatest likelihood [$\mathcal{L}(p) > \mathcal{L}(K)$ and $\mathcal{L}(p) > \mathcal{L}(\pi)$], while charged kaons and pions are discriminated based on comparing the likelihoods for these two hypotheses [$\mathcal{L}(K) > \mathcal{L}(\pi)$ or $\mathcal{L}(\pi) > \mathcal{L}(K)$].

Showers in the EMC not associated with any charged track are identified as photon candidates after fulfilling the following requirements. The deposited energy is required to be larger than 25 MeV in the barrel ($|\cos\theta| < 0.8$) region and 50 MeV in the end-cap region ($0.84 < |\cos\theta| < 0.92$). To suppress electronic noise and showers unrelated to the event, the EMC time deviation from the event start time is required to be within (0, 700) ns. The π^0 candidates are reconstructed from photon pairs, and their invariant masses are required to satisfy $115 < M(\gamma\gamma) < 150$ MeV/c^2. To improve momentum resolution, a mass-constrained fit to the π^0 nominal mass is applied to the photon pairs and the resulting energy and momentum of the π^0 are used for further analysis.

Candidates for K_S^0 and Λ are formed by combining two oppositely charged tracks into the final states $\pi^+\pi^-$ and $p\pi^-$. For these two tracks, their distances of closest approaches to the IP must be within ± 20 cm along the beam direction. No distance constraints in the transverse plane are required. The charged π is not subjected to the PID requirements described above, while proton PID is implemented in order to improve signal significance. The two daughter tracks are constrained to originate from a common decay vertex by requiring the χ^2 of the vertex fit to be less than 100. Furthermore, the decay vertex is required to be separated from the IP by a distance of at least twice the fitted vertex resolution. The fitted momenta of the $\pi^+\pi^-$ and $p\pi^-$ are used in the further analysis. We impose requirements $487 < M(\pi^+\pi^-) < 511$ MeV/c^2 and $1111 < M(p\pi^-) < 1121$ MeV/c^2 to select K_S^0 and Λ signal candidates, respectively, which are within about 3 standard deviations from their nominal masses. To form Σ^0, Σ^+ and ω candidates, requirements on the invariant masses of $1179 < M(\Lambda\gamma) < 1203$ MeV/c^2, $1176 < M(p\pi^0) < 1200$ MeV/c^2 and $760 < M(\pi^+\pi^-\pi^0) < 800$ MeV/c^2, are imposed.

When we reconstruct the decay modes $pK_S^0\pi^0$, $pK_S^0\pi^+\pi^-$ and $\Sigma^+\pi^+\pi^-$, possible backgrounds from $\Lambda \to p\pi^-$ in the final states are rejected by requiring $M(p\pi^-)$ outside the range $(1110, 1120)$ MeV/c^2. In addition, for the mode $pK_S^0\pi^0$, candidate events within the range $1170 < M(p\pi^0) < 1200$ MeV/c^2 are excluded to suppress Σ^+ backgrounds. To remove K_S^0 candidates in the modes $\Lambda\pi^+\pi^-\pi^+$, $\Sigma^+\pi^0$ and $\Sigma^+\pi^+\pi^-$, masses of any pairs of $\pi^+\pi^-$ and $\pi^0\pi^0$ are not allowed to fall in the range $(480, 520)$ MeV/c^2.

To discriminate Λ_c candidates from background, two variables reflecting energy and momentum conservation are used. First, we calculate the energy difference, $\Delta E \equiv E - E_{\text{beam}}$, where E is the total measured energy of the Λ_c candidate and E_{beam} is the average value of the e^+ and e^- beam energies. For each tag mode, candidates are rejected if they fail the ΔE requirements in Table I, which correspond to about 3 times the resolutions. Second, we define the beam-constrained mass M_{BC} of the Λ_c candidates by substituting the beam-energy E_{beam} for the energy E of the Λ_c candidates, $M_{\text{BC}}c^2 \equiv \sqrt{E_{\text{beam}}^2 - p^2c^2}$, where p is the measured Λ_c momentum in the center-of-mass system of the e^+e^- collision. Figure 1 shows the M_{BC} distributions for the ST samples, where evident Λ_c signals peak at the nominal Λ_c mass position (2286.46 ± 0.14) MeV/c^2 [4]. The MC simulations show that peaking backgrounds and cross feeds among the 12 ST modes are negligible.

We perform unbinned extended maximum likelihood fits to the M_{BC} distributions to obtain the ST yields, as illustrated in Fig. 1. In each fit, the signal shape is derived from MC simulations of the signal ST modes convolved with a Gaussian function to account for imperfect modeling of the detector resolution and beam-energy spread. The

TABLE I. Requirement on ΔE, ST yields, DT yields and detection efficiencies for each of the decay modes. The uncertainties are statistical only. The quoted efficiencies do not include any subleading BFs.

Mode	ΔE (MeV)	N_j^{ST}	$\varepsilon_j(\%)$	N_{i-}^{DT}	$\varepsilon_{i-}^{\mathrm{DT}}(\%)$
pK_S^0	$(-20, 20)$	1243 ± 37	55.9	97 ± 10	16.6
$pK^-\pi^+$	$(-20, 20)$	6308 ± 88	51.2	420 ± 22	14.1
$pK_S^0\pi^0$	$(-30, 20)$	558 ± 33	20.6	47 ± 8	6.8
$pK_S^0\pi^+\pi^-$	$(-20, 20)$	485 ± 29	21.4	34 ± 6	6.4
$pK^-\pi^+\pi^0$	$(-30, 20)$	1849 ± 71	19.6	176 ± 14	7.6
$\Lambda\pi^+$	$(-20, 20)$	706 ± 27	42.2	60 ± 8	12.7
$\Lambda\pi^+\pi^0$	$(-30, 20)$	1497 ± 52	15.7	101 ± 13	5.4
$\Lambda\pi^+\pi^-\pi^+$	$(-20, 20)$	609 ± 31	12.0	53 ± 7	3.6
$\Sigma^0\pi^+$	$(-20, 20)$	522 ± 27	29.9	38 ± 6	9.9
$\Sigma^+\pi^0$	$(-50, 30)$	309 ± 24	23.8	25 ± 5	8.0
$\Sigma^+\pi^+\pi^-$	$(-30, 20)$	1156 ± 49	24.2	80 ± 9	8.1
$\Sigma^+\omega$	$(-30, 20)$	157 ± 22	9.9	13 ± 3	3.8

parameters of the Gaussians are allowed to vary in the fits. Backgrounds for each mode are described with the ARGUS function [16]. The resultant ST yields in the signal region $2276 < M_{\mathrm{BC}} < 2300$ MeV/c^2 and the corresponding detection efficiencies are listed in Table I.

In the signal candidates of the 12 ST modes, a specific mode $\Lambda_c^+ \to i$ is formed from the remaining tracks and showers recoiling against the ST $\bar{\Lambda}_c^-$. We combine the DT signal candidates over the 12 ST modes and plot the distributions of the M_{BC} variable in Fig. 2. We follow the same fit strategy as in the ST samples to estimate the total DT yield N_{i-}^{DT} in Eq. (4), except that the DT signal shapes are derived from the DT signal MC samples and convolved

with the Gaussian function. The parameters of the Gaussians are also allowed to vary in the fits. The extracted DT yields are listed in Table I. The 12×12 DT efficiencies ε_{ij} are evaluated based on the DT signal MC samples, in order to extract the BFs.

Main sources of systematic uncertainties related to the measurement of BFs include tracking, PID, reconstruction of intermediate states and intermediate BFs. For the ΔE and M_{BC} requirements, the uncertainties are negligible, as we correct resolutions in MC samples to accord with those in data. Uncertainties associated with the efficiencies of the tracking and PID of charged particles are estimated by studying a set of control samples of $e^+e^- \to \pi^+\pi^+\pi^-\pi^-$, $K^+K^-\pi^+\pi^-$ and $p\bar{p}\pi^+\pi^-$ based on data taken at energies above $\sqrt{s} = 4.0$ GeV. An uncertainty of 1.0% is assigned to each π^0 due to the reconstruction efficiency. The uncertainties of detecting K_S^0 and Λ are determined to be 1.2% and 2.5%, respectively. Reweighting factors for the 12 signal models are varied within their statistical uncertainties obtained from the ST data samples. Deviations of the resultant efficiencies are taken into account in systematic uncertainties. Systematic uncertainties due to limited statistics in MC samples are included. Uncertainties on the BFs of intermediate state decays from the PDG [4] are also included. A summary of systematic uncertainties are given in Table II.

We use a least-squares fitter, which considers statistical and systematic correlations among the different hadronic modes, to obtain the BFs of the 12 Λ_c^+ decay modes globally. Details of this fitter are discussed in Ref. [17]. In the fitter, the precisions of the 12 BFs are constrained to a common variable, $N_{\Lambda_c^+\bar{\Lambda}_c^-}$, according to Eqs. (1) and (4). In total, there are 13 free parameters (12 $\mathcal{B}_i$ and $N_{\Lambda_c^+\bar{\Lambda}_c^-}$) to be
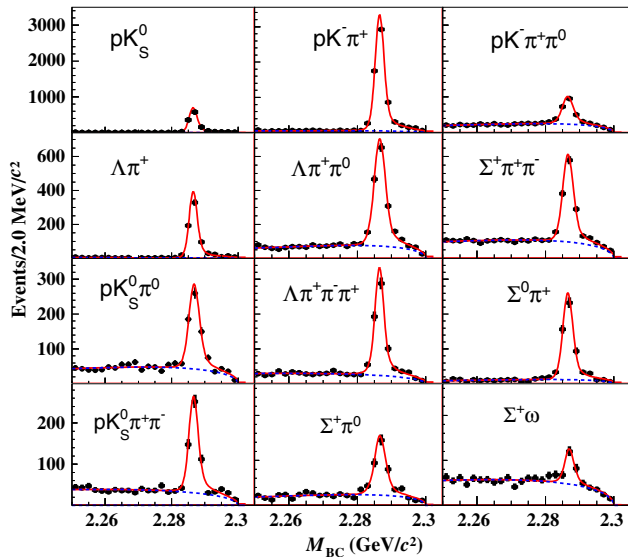

FIG. 1. Fits to the ST M_{BC} distributions in data for the different decay modes. Points with error bars are data, solid lines are the sum of the fit functions, and dashed lines are the background shapes.
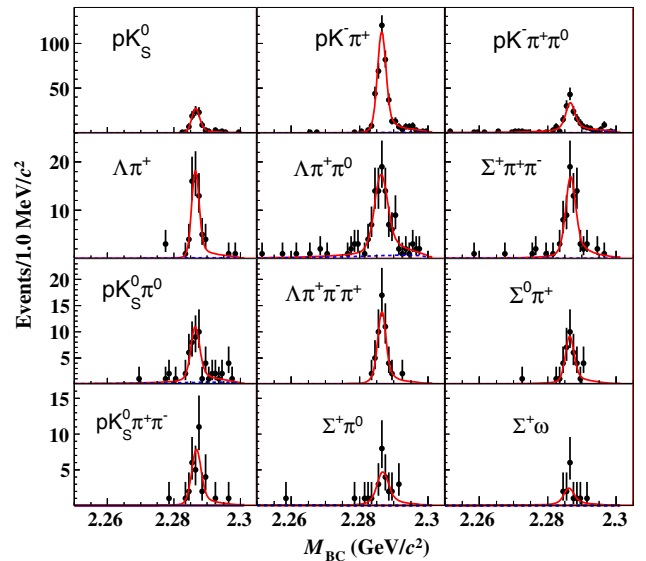

FIG. 2. Fits to the DT M_{BC} distributions in data for different signal modes. Points with error bars are data, solid lines are the sum of fit functions, and dashed lines are background shapes.

TABLE II. Summary of systematic uncertainties, in percent. The total numbers are derived from the least-squares fit, by taking into account correlations among different modes.

Source	Tracking	PID	K_S^0	Λ	π^0	Signal model	MC stat	Quoted BFs	Total
pK_S^0	1.3	0.3	1.2			0.2	0.4	0.1	2.0
$pK^-\pi^+$	2.5	3.2					0.2		3.9
$pK_S^0\pi^0$	1.1	1.6	1.2		1.0	1.0	0.5	0.1	2.7
$pK_S^0\pi^+\pi^-$	2.8	5.4	1.2			0.5	0.5	0.1	5.9
$pK^-\pi^+\pi^0$	3.3	5.8			1.0	2.0	0.5		6.6
$\Lambda\pi^+$	1.0	1.0		2.5		0.5	0.5	0.8	2.4
$\Lambda\pi^+\pi^0$	1.0	1.0		2.5	1.0	0.6	0.6	0.8	2.7
$\Lambda\pi^+\pi^-\pi^+$	3.0	3.0		2.5		0.8	0.8	0.8	4.7
$\Sigma^0\pi^+$	1.0	1.0		2.5		1.7	0.7	0.8	2.4
$\Sigma^+\pi^0$	1.3	0.3			2.0	1.7	0.8	0.1	2.5
$\Sigma^+\pi^+\pi^-$	3.0	3.7			1.0	0.8	0.4	0.1	4.7
$\Sigma^+\omega$	3.0	3.2			2.0	7.1	1.0	0.8	4.5

estimated. As peaking backgrounds in ST modes and cross feeds among the 12 ST modes are suppressed to a negligible level, they are not considered in the fit.

The extracted BFs of Λ_c^+ are listed in Table III; the correlation matrix is available in the Supplemental Material [18]. The total number of $\Lambda_c^+\bar{\Lambda}_c^-$ pairs produced is obtained to be $N_{\Lambda_c^+\bar{\Lambda}_c^-} = (105.9 \pm 4.8 \pm 0.5) \times 10^3$. The goodness-of-fit is evaluated as $\chi^2/\text{ndf} = 9.9/(24 - 13) = 0.9$.

To summarize, 12 Cabibbo-favored Λ_c^+ decay rates are measured by employing a double-tag technique, based on a sample of threshold data at $\sqrt{s} = 4.599$ GeV collected at BESIII. This is the first absolute measurement of the Λ_c^+ decay branching fractions at the $\Lambda_c^+\bar{\Lambda}_c^-$ production threshold, in the 30 years since the Λ_c^+ discovery. A comparison with previous results is presented in Table III. For the golden mode $\mathcal{B}(pK^-\pi^+)$, our result is consistent with that in PDG, but lower than Belle's with a significance of about 2σ. For the branching fractions of the other modes,

TABLE III. Comparison of the measured BFs in this work with previous results from PDG [4]. For our results, the first uncertainties are statistical and the second are systematic.

Mode	This work (%)	PDG (%)
pK_S^0	$1.52 \pm 0.08 \pm 0.03$	1.15 ± 0.30
$pK^-\pi^+$	$5.84 \pm 0.27 \pm 0.23$	5.0 ± 1.3
$pK_S^0\pi^0$	$1.87 \pm 0.13 \pm 0.05$	1.65 ± 0.50
$pK_S^0\pi^+\pi^-$	$1.53 \pm 0.11 \pm 0.09$	1.30 ± 0.35
$pK^-\pi^+\pi^0$	$4.53 \pm 0.23 \pm 0.30$	3.4 ± 1.0
$\Lambda\pi^+$	$1.24 \pm 0.07 \pm 0.03$	1.07 ± 0.28
$\Lambda\pi^+\pi^0$	$7.01 \pm 0.37 \pm 0.19$	3.6 ± 1.3
$\Lambda\pi^+\pi^-\pi^+$	$3.81 \pm 0.24 \pm 0.18$	2.6 ± 0.7
$\Sigma^0\pi^+$	$1.27 \pm 0.08 \pm 0.03$	1.05 ± 0.28
$\Sigma^+\pi^0$	$1.18 \pm 0.10 \pm 0.03$	1.00 ± 0.34
$\Sigma^+\pi^+\pi^-$	$4.25 \pm 0.24 \pm 0.20$	3.6 ± 1.0
$\Sigma^+\omega$	$1.56 \pm 0.20 \pm 0.07$	2.7 ± 1.0

the precisions are improved by factors of 3–6 compared to the world average values.

[a]Also at State Key Laboratory of Particle Detection and Electronics, Beijing 100049, Hefei 230026, People's Republic of China.
[b]Also at Bogazici University, 34342 Istanbul, Turkey.
[c]Also at the Moscow Institute of Physics and Technology, Moscow 141700, Russia.
[d]Also at the Functional Electronics Laboratory, Tomsk State University, Tomsk 634050, Russia.
[e]Also at the Novosibirsk State University, Novosibirsk 630090, Russia.
[f]Also at the NRC "Kurchatov Institute", PNPI, 188300 Gatchina, Russia.
[g]Also at University of Texas at Dallas, Richardson, Texas 75083, USA.
[h]Also at Istanbul Arel University, 34295 Istanbul, Turkey.
[i]Corresponding author.
lipeirong11@mails.ucas.ac.cn

[j]Corresponding author.
xiaorui@ucas.ac.cn

[1] J. L. Rosner, Phys. Rev. D **86,** 014017 (2012).

[2] S. A. Dytman *et al.* (CLEO Collaboration), Phys. Rev. D **66,** 091101 (2002).

[3] P. Abreu *et al.* (DELPHI Collaboration), Eur. Phys. J. C **12,** 225 (2000); R. Barate *et al.* (ALEPH Collaboration), Eur. Phys. J. C **16,** 597 (2000); R. Aaij *et al.* (LHCb Collaboration), Phys. Rev. D **85,** 032008 (2012).

[4] K. A. Olive *et al.* (Particle Data Group), Chin. Phys. C **38,** 090001 (2014).

[5] D. E. Jaffe *et al.* (CLEO Collaboration), Phys. Rev. D **62,** 072005 (2000).

[6] A. Zupanc *et al.* (Belle Collaboration), Phys. Rev. Lett. **113,** 042002 (2014).

[7] M. Ablikim *et al.* (BESIII Collaboration), Chin. Phys. C **39,** 093001 (2015)

[8] M. Ablikim *et al.* (BESIII Collaboration), Nucl. Instrum. Methods Phys. Res., Sect. A **614,** 345 (2010).

[9] R. M. Baltrusaitis (MARK-III Collaboration), Phys. Rev. Lett. **56,** 2140 (1986); J. Adler *et al.* (MARK-III Collaboration), Phys. Rev. Lett. **60,** 89 (1988).

[10] M. Ablikim *et al.* (BESIII Collaboration), Phys. Rev. Lett. **115,** 221805 (2015).

[11] The$\Sigma^+\pi^+\pi^-\pi^0$ mode suffers from huge combinatorial backgrounds. We restrict $\pi^+\pi^-\pi^0$ from ω decays and only measure the resonant component $\Sigma^+\omega$, where the nonresonant final states $\Sigma^+\pi^+\pi^-\pi^0$ are negligible.

[12] S. Jadach, B. F. L. Ward, and Z. Was, Phys. Rev. D **63,** 113009 (2001).

[13] N. Brambilla *et al.*, Eur. Phys. J. C **71,** 1534 (2011).

[14] D. J. Lange, Nucl. Instrum. Methods Phys. Res., Sect. A **462,** 152 (2001); R. G. Ping, Chin. Phys. C **32,** 599 (2008).

[15] S. Agostinelli *et al.* (GEANT Collaboration), Nucl. Instrum. Methods Phys. Res., Sect. A **506,** 250 (2003); J. Allison *et al.*, IEEE Trans. Nucl. Sci. **53,** 270 (2006).

[16] H. Albrecht *et al.* (ARGUS Collaboration), Phys. Lett. B **241,** 278 (1990).

[17] Y. Guan, X. R. Lu, Y. Zheng, and Y. S. Zhu, Chin. Phys. C **37,** 106201 (2013).

[18] See Supplemental Material at http://link.aps.org/supplemental/10.1103/PhysRevLett.116.052001 for the correlation matrix of the fit.